

Published in final edited form as:

Bioorg Med Chem Lett. 2014 August 15; 24(16): 3719–3723. doi:10.1016/j.bmcl.2014.07.011.

Physicochemical Property-Driven Optimization of Diarylaniline Compounds as Potent HIV-1 Non-Nucleoside Reverse Transcriptase Inhibitors

Na Liu^a, Bingjie Qin^a, Lian-Qi Sun^a, Fei Yu^{b,c}, Lu Lu^b, Shibo Jiang^{b,c}, Kuo-Hsiung Lee^{d,e,*}, and Lan Xie^{a,*}

^aBeijing Institute of Pharmacology & Toxicology, 27 Tai-Ping Road, Beijing, 100850, China

^bKey Laboratory of Medical Molecular Virology of Ministries of Education and Health, Shanghai Medical College and Institute of Medical Microbiology, Fudan University, Shanghai 200032, China

^cLindsley F. Kimball Research Institute, New York Blood Center, NY 10065, USA

^dNatural Products Research Laboratories, UNC Eshelman School of Pharmacy, University of North Carolina, Chapel Hill, NC 27599-7568, USA

^eChinese Medicine Research and Development Center, China Medical University and Hospital, Taichung, Taiwan

Abstract

Using physicochemical property-driven optimization, twelve new diarylaniline compounds (DAANs) (**7a–h**, **11a–b** and **12a–b**) were designed and synthesized. Among them, compounds **12a–b** not only showed high potency (EC₅₀ 0.96–4.92 nM) against both wild-type and drug-resistant viral strains with the lowest fold change (FC 0.91 and 5.13), but also displayed acceptable drug-like properties based on aqueous solubility and lipophilicity (LE > 0.3, LLE > 5, LELP < 10). The correlations between potency and physicochemical properties of these DAAN analogues are also described. Compounds **12a–b** merit further development as potent clinical trial candidates against AIDS.

Keywords

anti-HIV agents; diarylaniline; NNRTIs; physicochemical property

Non-nucleoside reverse transcriptase inhibitors (NNRTIs) with diverse structures are a key component of antiretroviral therapy (ART) for HIV infection and AIDS, because they exhibit high efficacy and low toxicity, as well as synergistic activity in combination with

© 2014 Elsevier Ltd. All rights reserved.

*Corresponding author, lanxie4@gmail.com; Tel/Fax: 86-10-66931690 (L. Xie); khlee@unc.edu; Tel: 919-962-0066; Fax: 919-966-3893.

Publisher's Disclaimer: This is a PDF file of an unedited manuscript that has been accepted for publication. As a service to our customers we are providing this early version of the manuscript. The manuscript will undergo copyediting, typesetting, and review of the resulting proof before it is published in its final citable form. Please note that during the production process errors may be discovered which could affect the content, and all legal disclaimers that apply to the journal pertain.

other anti-HIV drugs.^{1,2} Two new-generation NNRTIs, etravirine (TMC125, **1a**) and rilpivirine (TMC278, **1b**) (Fig. 1), which were recently approved by the FDA for anti-AIDS therapy, have much better potency and pharmacological profiles than early NNRTIs, such as nevirapine, delavirdine, and efavirenz, and can efficiently inhibit a broad spectrum of drug-resistant viral strains.³ However, clinical trials revealed novel resistance mutations⁴ conferred against drugs **1a** and **1b**, which are both diarylpyrimidine (DAPY) compounds, similar to the early NNRTIs. However, these newly produced resistance mutations differ from those affecting the early NNRTIs and from each other, suggesting that a subtle structural difference between the drugs was sufficient to cause the occurrence of distinct HIV mutations. This discovery underscores the necessity for developing new NNRTI drugs with diverse scaffolds in order to provide more choices for AIDS treatment and overcome new resistance mutants. Accordingly, a number of new-generation NNRTI agents with diverse structures have been discovered⁵ and are currently undergoing preclinical and clinical trials.

In our prior studies, several diarylanilines (DAANs) were identified as novel class of HIV-1 non-nucleoside reverse transcriptase inhibitor (NNRTI) agents with low nanomolar anti-HIV potency against wild-type and mutated viral strains^{6,7}, both comparable to and better than new-generation NNRTI drugs **1a** and **1b**. These DAANs are shown in Figure 1 as leads **2a** and **2b**. However, their poor aqueous solubility (< 1 µg/mL) resulted in very low absorption *in vivo*. To improve molecular aqueous solubility, several polar groups^{8,9}, including carboxyl, ester, amide, hydroxyl, and CF₃, were introduced at the R¹ group on the central phenyl ring, a point known to be modifiable for anti-HIV potency, while also associated with molecular physicochemical properties. These efforts led to the discovery of hydroxymethyl-DAAN **2c** (Fig. 1) with high potency against wild-type and multi drug-resistant viral strains (EC₅₀ 0.53 nM and 0.4 nM, respectively) and improved aqueous solubility of 3.23 µg/mL at pH 7.4 and 20.9 µg/mL at pH 2.0. Unfortunately, **2c** displayed low oral bioavailability (F% 6.10) in pharmacokinetics assays *in vivo*. Herein, we have again modified the DAAN compounds to identify potential drug candidates with balanced potency and a desirable absorption, distribution, metabolism, and excretion (ADME) profile.

To explore the correlations between potency and physicochemical properties associated with ADME profile, we continued to focus on the R¹ substituent on the central phenyl ring. In our newly designed series of DAAN analogues (**7a–h**, **11a–b**, **12a–b**), R¹ was altered to alkylamines or alkoxyethers with different shapes, lengths or volumes. After anti-HIV evaluations, the new active DAAN compounds were further assessed for multiple physicochemical properties, including aqueous solubility and lipophilicity, as estimated by log P. Apart from aqueous solubility, lipophilicity is another major physicochemical property that contributes to potency, affects compound solubility, determines the passive permeability of small molecules through biological membranes, impacts drug metabolism and pharmacokinetics, and influences adverse effects and compound-related toxicity. Most recently, new lipophilic parameters, *i.e.*, lipophilic efficiency (LE), lipophilic ligand efficiency (LLE),¹⁰ and ligand-efficiency-dependent lipophilicity (LELP),¹¹ have been proposed and applied in many medicinal chemistry programs^{12,13,14} to efficiently guide lead optimization. Herein, the synthesis, anti-HIV potency, and assessments of multiple

physicochemical properties of three series of new DAAN compounds (**7a–h**, **11a–b**, **12a–b**) are reported. The results will be helpful in guiding our further lead optimization aimed at the discovery of new clinical trial candidates as potent anti-AIDS drugs.

As shown in Scheme 1, target DAAN compounds **7a–h** were prepared through a short synthetic route, starting from commercially available 4-hydroxy-3,5-dimethylbenzotrile (**3**). The previously synthesized intermediate 5-chloro-*N*¹-(4-cyanophenyl)-4-methoxycarbonyl-2-nitroaniline (**4**)⁸ was coupled with **3** in the presence of potassium carbonate in DMF under 120 °C for 6 h to afford 2,4-diarylnitrobenzene **5**. By using lithium borohydride (LiBH₄), the ester group on the central phenyl ring in **5** was reduced to a hydroxymethyl group in the key intermediate **6a**. Subsequently, **6a** was treated with 2,4,6-trichloro-[1,3,5]triazine followed by nucleophilic substitution with methylamine, cyclopropanamine, 3-aminopropan-1-ol, or 1-methyl-piperazine to produce the corresponding compounds **6b–e**, respectively, with different alkylamines at the R¹ position. Alternatively, **6a** was reacted with isopropanol or methanol in the presence of bismuth chloride (BiCl₃) to afford the corresponding alkoxyethyl-DAAN compounds **6f** and **6g**. Furthermore, the hydroxyl group in **6a** was esterified with acetic anhydride to yield compound **6h**. Finally, the nitro group on the central ring of **6a–h** was reduced via catalytic hydrogenation in the presence of Pd-C (10%) in either EtOAc or anhydrous ethanol to furnish new DAAN compounds **7a–h**. The structures of these new DAAN compounds were identified from proton NMR and MS spectra.¹⁵

Newly synthesized DAAN compounds **7a–h** were initially evaluated against wild-type HIV-1 (IIIB) replication in MT-2 cells in parallel with drug **1b**. The data are presented in Table 1. As expected, most new DAANs, except **7e** with a bulky *N*-methylpiperazinyl group at the R¹ position (EC₅₀ 170 nM), exhibited low nanomolar potency with EC₅₀ values ranging from 1.06 to 14 nM and high selective index (SI) values of 1,142 to 114,019. The new **7**-series compounds were also evaluated against K103N/Y181C mutant-derived, NNRTI-resistant viral strain A17. However, their potencies against the wild-type viral strain were clearly reduced, as demonstrated by EC₅₀ values of greater than 33 to 2,000 nM.

Based on previous SAR results,⁹ we then designed and synthesized two pairs of compounds **11a–b** and **12a–b** with a *para*-cyanovinyl and *para*-cyanoethyl (R²) group, respectively, on the phenoxy ring (C-ring), as shown in Scheme 2. Similarly to the preparation of **7g** and **7h**, methoxymethyl-DAAN **9** and acetoxymethyl-DAAN **10** were synthesized from *N*¹-(4-cyanophenyl)-5-(4'-cyanovinyl-2',6'-dimethylphenoxy)-4-hydroxymethyl-2-nitroaniline (**8**).⁹ Subsequently, the nitro group in **9** and **10** was reduced with iron powder in the presence of NH₄Cl to afford corresponding *para*-cyanovinyl-DAAN compounds **11a** and **11b**,¹⁵ respectively, while the nitro group (R¹) and the conjugated double bond in the cyanovinyl group (R²) of **9** and **10** were reduced simultaneously using catalytic hydrogenation with Pd/C to produce *para*-cyanoethyl-DAAN compounds **12a** and **12b**.¹⁵ The two pairs of compounds, **11a–b** and **12a–b**, exhibited high potency against wild-type HIV-1 replication with sub- to low nanomolar EC₅₀ values ranging from 0.83 to 5.74 nM, and were as or more potent than **7g** and **7h**, regardless of whether R² was *p*-cyanovinyl or *p*-cyanoethyl. More importantly, compounds **12a–b** showed high potency against resistant

viral strain A17. Specifically, cyanoethyl-DAAN **12a** (EC₅₀ 2.95 nM) was more potent than cyanovinyl-DAAN **11a** (14.7 nM), while both were more potent than cyano-DAAN compound **7g** (298 nM). Similar differences in potency were observed when comparing acetoxymethyl-DAAN compounds **12b** (4.92 nM), **11b** (36.5 nM), and **7h** (374 nM). These results clearly demonstrate that the R² group on the phenoxy ring (C-ring) directly affects molecular potency against wild-type, as well as resistant, viral strains. A cyanoethyl group, which is more flexible due to its linearity, was more favorable than a cyanovinyl or cyano group. Notably, highly potent **12a** and **12b** had low fold change (FC) between A17 and wild-type IIIB virus with FC values of 0.91 and 5.13, respectively, much lower than that of **1b** (FC 18.4) in the same assay.

Next, several physicochemical properties of newly generated DAANs (EC₅₀ < 11 nM) (**7a–d**, **7g–h**, **11a–b**, **12a–b**) and drug **1b** were assessed, and the resulting data are summarized in Table 2. Aqueous solubility was measured by HPLC at pH 2.0 and 7.4 to reflect the physiological conditions encountered by these compounds in stomach and plasma, respectively. As expected, alkylamine-DAAN compounds **7b**, **7c**, and **7d** displayed greatly improved solubility at both pH 2.0 (263, 285, and 290 µg/mL, respectively) and pH 7.4 (159, 13, and 236 µg/mL, respectively) compared with drug **1b** (pH 2.0, 74 µg/mL; pH 7.4, 0.29 µg/mL). Thus, the introduction of suitable alkylamino groups at the R¹ position could greatly improve the molecular aqueous solubility. Active compounds hydroxymethyl-DAAN **7a** (R¹ = CH₂OH), methoxymethyl-DAANs **7g**, **11a**, and **12a** (R¹ = CH₂OMe), and acetoxymethyl-DAANs **7h**, **11b**, and **12b** (R¹ = CH₂OAc) also demonstrated improved aqueous solubility at pH 2.0 (1.7–9.10 µg/mL), but not at pH 7.4 (< 1 µg/mL). For oral drug candidates, better aqueous solubility at pH 2.0 is desirable to enhance absorbability in the stomach.¹⁸ Meanwhile, we observed that all 10 new active compounds had lower melting points than **1b**. This difference might be explained by the assumption that the R¹ group on the central phenyl ring might disrupt molecular planarity and crystal packing,¹⁹ which could also enhance molecular aqueous solubility. To estimate molecular lipophilicity, the log P parameters of these active compounds were measured by HPLC at pH 7.4.⁹ The experimental log P values fell within an acceptable range of 1.80–4.40, which is consistent with the measured aqueous solubilities, and showed the same trend as the clog D values predicted by ACD software. Additionally, topological polar surface area (tPSA) parameters of all active compounds were calculated by ChemDraw Ultra 12.0 and met the criterion²⁰ of < 140 Å² for potential oral drug candidates.

To estimate the possible ADME profiles and potential of our drug candidates, we focused next on their lipophilic indices, including lipophilic efficiency (LE), lipophilic ligand efficiency (LLE), and ligand-efficiency-dependent lipophilicity (LELP). Defined as the difference between the negative logarithm of the measured potency (pEC₅₀) and log P, LLE quantifies the contribution of lipophilicity to potency, whereas LELP¹⁷ correlates with ADME properties. Thus, compounds with a low LELP value would most likely have a high chance of passing all ADME and safety criteria,²¹ while compounds with high LELP values (typically > 10) would have a higher propensity to fail because of ADME and safety risks. Accordingly, lipophilic parameters of the new active DAANs were calculated from their experimental EC₅₀ and log P values by the formulas cited at the bottom of Table 2.

Consequently, compounds **7a**, **7b**, **7d**, **12a**, and **12b** met acceptable levels for all three ligand lipophilic-efficiency indices ($LE > 0.3$, $LLE > 5$, $LLEP < 10$),²¹ while the remaining compounds in Table 2 did not, having either LLE values lower than 5 or LLEP values higher than 10. Among the five promising compounds, **7b** and **7d** showed higher aqueous solubility at different pH conditions as well as lower log P and LLEP values than the other compounds, suggesting better ADME profiles. On the other hand, the **7** series of DAANs were not efficient against resistant viral strain A17. Compounds **12a** and **12b** did show more balanced potency between the HIV-1 wild-type and resistant viral strains, as well as met acceptable lipophilic criteria, as determined by the LE, LLE and LLEP indices. However, the aqueous solubility of both compounds was obviously lower than that of either **7b** or **7d**. Thus, to avoid the risk of potential oral absorption, these results suggested that the **12a–b** pair requires additional optimization to improve aqueous solubility.

In summary, three series of new DAAN compounds (**7a–h**, **11a–b**, and **12a–b**) with interchangeable R¹ and R² modification/optimization were successfully synthesized as part of our ongoing anti-HIV NNRTI program. Our current physicochemical property-driven optimization resulted in the discovery of two promising compounds, **12a** and **12b**, with high potency against wild-type and drug-resistant viral strains, low nanomolar EC₅₀ values (0.96–4.92 nM), low fold change resistance (FC 0.91 and 5.13), and acceptable lipophilicity, as demonstrated by meeting acceptable values for all lipophilic parameters ($LE > 0.3$, $LLE > 5$, $LLEP < 10$; $\log P < 5$, $tPSA < 140 \text{ \AA}^2$)²¹, even though their aqueous solubility needs further improvement. Optimization of the series **7** compounds revealed that (1) the presence of an alkylamine substituent at the R¹ position can greatly improve molecular aqueous solubility (see **7b–d**) without loss of antiviral potency, (2) a bulky R¹ group can result in substantially impaired antiviral activity (see **7e**), and (3) introducing an H-bond acceptor or donor at the R¹ position (such as **7a–b**, **7d–g**) might regulate the molecular lipophilicity to meet desired drug criteria. Our optimization efforts at the R² position on the phenoxy ring (C-ring) indicated that a more flexible and longer linear cyanovinyl (**11** series) or, preferably, cyanoethyl (**12** series) substituent, rather than a cyano group (**7** series) is crucial for high potency against both wild-type and double-mutant drug-resistant viral strains (compare **7g–h**, **11a–b**, and **12a–b**). Consequently, a number of compounds from this series are being considered for *in vivo* pharmacokinetic evaluation, and the results will be reported later.

Acknowledgments

This investigation was supported by grants 30930106 and 81120108022 from the Natural Science Foundation of China (NSFC) to L. Xie, the National Megaprojects of China for Major Infectious Diseases (2013ZX10001-006) to L. Xie and S. Jiang, and U.S. NIH grant (AI33066) to K. H. Lee. This study was also supported in part by the Taiwan Department of Health, China Medical University Hospital Cancer Research Center of Excellence (DOH100-TD-C-111-005).

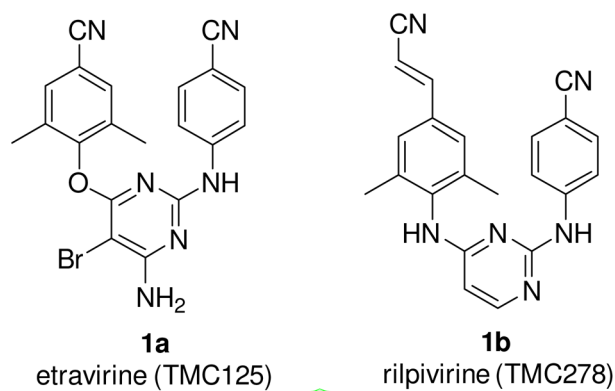
References and Notes

1. Tronchet JM, Seman M. *Curr Top Med Chem.* 2003; 3:1496. [PubMed: 14529523]
2. Tarby CM. *Curr Top Med Chem.* 2004; 4:1045. [PubMed: 15193138]
3. Guillemont J, Pasquier E, Palandjian P, Vemier D, Gaurrand S, Lewi PJ, Heeres J, De Jonge MR, Koymans LMH, Daeyaert FFD, Vinkers MH, Arnold E, Das K, Pauwels R, Andries K, De Bethune

- M-P, Bettens E, Hertogs K, Wigerinck P, Timmerman P, Janssen PA. *J Med Chem.* 2005; 48:2072. [PubMed: 15771449]
4. Bourgeois A, Womack S, Newsom D, Caldwell D. *HIV Clinician.* 2012; 24:12. [PubMed: 23259177]
 5. Rawal RK, Murugesan V, Katti SB. *Curr Med Chem.* 2012; 19:5364. [PubMed: 22998569]
 6. Qin B, Jiang XK, Lu H, Tian XT, Barbault F, Huang L, Qian K, Chen CH, Huang R, Jiang S, Lee KH, Xie L. *J Med Chem.* 2010; 53:4906. [PubMed: 20527972]
 7. Tian XT, Qin B, Wu ZY, Wang XF, Lu H, Morris-Natschke SL, Chen CH, Jiang S, Lee KH, Xie L. *J Med Chem.* 2010; 53:8287. [PubMed: 21049929]
 8. Sun LQ, Qin B, Huang L, Qian K, Chen CH, Lee KH, Xie L. *Bioorg Med Chem Lett.* 2012; 22:2376. [PubMed: 22406117]
 9. Sun LQ, Zhu L, Qian K, Qin B, Huang L, Chen CH, Lee KH, Xie L. *J Med Chem.* 2012; 55:7219. [PubMed: 22856541]
 10. Leeson PD, Springthorpe B. *Nat Rev Drug Discovery.* 2007; 6:881.
 11. Keseru GM, Makara GM. *Nat Rev Drug Discovery.* 2009; 8:203.
 12. Jabeen I, Plehab K, Rinner U, Chibe P, Ecker GF. *J Med Chem.* 2012; 55:3261. [PubMed: 22452412]
 13. Christiansen E, Due-Hansen ME, Urban C, Grundmann M, Schroder R, Hudson BD, Milligan G, Cawthorne MA, Kostenis E, Kassack MU, Ulven T. *J Med Chem.* 2012; 55:6624. [PubMed: 22724451]
 14. Diaz JL, Christmann U, Fernandez A, Luengo M, Bordas M, Enrech R, Carro M, Pascual R, Burgueno J, Merlos M, Bebet-Buchholz J, Ceron-Bertran J, Ramirez J, Reinoso RF, de Henestrosa FAR, Vela JM, Almansa C. *J Med Chem.* 2013; 56:3656. [PubMed: 23560650]
 15. Synthetic procedure for 4-substituted 1,5-diarylbenzene-1,2-diamines (**7a–h** and **12a–b**). A solution of diarylnitrobenzene in 20 mL of anhydrous EtOAc (for **7a–c**, **7e–f**) or anhydrous EtOH (for **7d**, **7g–h**, **12a–b**) in the presence of excess Pd/C (5%) was shaken with hydrogen gas under 50–55 p.s.i. until the hydrogen was no longer absorbed (ca. 4 h). The catalyst was filtered from the solution and washed with EtOAc several times. After the solvent was removed under reduced pressure, the residue was purified by flash column chromatography (gradual elution: MeOH/CH₂Cl₂, 0–5%) with the Combiflash® flash chromatography system (Teledyne ISCO Company, Inc., Lincoln, NE) to obtain pure target compounds **7a–h** and **12a–b**. Otherwise, *para*-cyanovinyl-compounds **11a** and **11b** were obtained from **9** and **10** by reaction with excess iron powder in the presence of NH₄Cl at reflux temperature in a mixed solvent of THF/MeOH (v/v/v 1:1:1) for 4 h. **7a**: yield 73%, white solid, mp 230.0–232 °C; ¹H NMR (CDCl₃) δ ppm 2.14 (6H, s, 2 × CH₃), 4.88 (2H, s, CH₂), 5.51 (1H, s, NH) 5.99 (1H, s, ArH-6), 6.54 (2H, d, *J* = 8.4 Hz, ArH-2',6'), 6.97 (1H, s, ArH-3), 7.40 (2H, s, ArH-3'',5''), 7.41 (2H, d, *J* = 8.4 Hz, ArH-3',5'); MS *m/z* (%) 385.2 (M + 1, 100). **7b**: white solid, mp 201–203 °C; ¹H NMR (CDCl₃) δ ppm 2.13 (6H, s, 2 × CH₃), 2.56 (3H, s, NCH₃), 3.58 (2H, s, NH₂), 3.95 (2H, s, ArCH₂), 5.51 (1H, s, NH), 5.96 (1H, s, ArH-6), 6.53 (2H, d, *J* = 8.4 Hz, ArH-2',6'), 6.93 (1H, s, ArH-3), 7.38 (2H, s, ArH-3'',5''), 7.39 (2H, d, *J* = 8.4 Hz, ArH-3',5'); MS *m/z* (%) 398.1 (M + 1, 1), 358 (M – 30, 100). **7c**: yield 83%, white solid, mp 72.0–73.3 °C; ¹H NMR (CDCl₃) δ ppm 0.49 (4H, m, CH₂CH₂), 2.14 (6H, s, 2 × CH₃), 2.24 (3H, m, CH), 3.53 (2H, s, NH₂), 4.00 (2H, s, ArCH₂), 5.48 (1H, s, NH), 5.96 (1H, s, ArH-6), 6.53 (2H, d, *J* = 8.8 Hz, ArH-2',6'), 6.93 (1H, s, ArH-3), 7.38 (2H, s, ArH-3'',5''), 7.39 (2H, d, *J* = 8.8 Hz, ArH-3',5'); MS *m/z* (%) 434.2 (M + 1, 3), 367.2 (M – 56, 100). **7d**: yield 38%, white solid, mp 76.0–78.0 °C; ¹H NMR (CDCl₃) δ ppm 1.79 (2H, f, *J* = 5.6 Hz, CH₂), 2.13 (6H, s, 2 × CH₃), 3.01 (2H, t, *J* = 5.6 Hz, NCH₂), 3.87 (2H, t, *J* = 5.6 Hz, CH₂O), 3.95 (2H, s, ArCH₂), 5.51 (1H, s, NH), 5.96 (1H, s, ArH-6), 6.54 (2H, d, *J* = 8.8 Hz, ArH-2',6'), 6.86 (1H, s, ArH-3), 7.39 (2H, s, ArH-3'',5''), 7.41 (2H, d, *J* = 8.8 Hz, ArH-3',5'); MS *m/z* (%) 442.6 (M + 1, 20), 367.2 (M – 74, 100). **7e**: yield 40%, white solid, mp 210.2–212.0 °C; ¹H NMR (CDCl₃) δ ppm 2.09 (3H, s, CH₃), 2.08 (3H, s, CH₃), 2.12 (6H, s, 2 × CH₃), 2.78 (4H, t, *J* = 4.8 Hz, CH₂CH₂), 3.05 (4H, s, *J* = 4.8 Hz, CH₂CH₂), 3.72 (2H, s, ArCH₂), 5.87 (1H, s, NH), 6.01 (1H, s, ArH-3), 6.60 (2H, d, *J* = 8.4 Hz, ArH-2',6'), 7.44 (2H, d, *J* = 8.4 Hz), 7.69 (2H, s, ArH-3'',5''), 8.62 (1H, s, ArH-6); MS *m/z* (%) 467.6 (M + 1, 31), 367.3 (M – 99, 100). **7f**: yield 33%, white solid, mp 140.9–142.9 °C; ¹H NMR (CDCl₃) δ ppm 1.28 (6H, d, *J* = 6.4 Hz, 2 × CH₃), 2.14 (6H, s, 2 × CH₃), 3.81 (1H, q, *J* = 6.4 Hz, CH), 4.69 (2H, s, ArCH₂), 5.53 (1H, s, NH), 5.96 (1H, s, ArH-6), 6.53 (2H, d, *J* =

8.4 Hz, ArH-2',6'), 7.04 (1H, s, ArH-3), 7.38 (2H, s, ArH-3'',5''), 7.40 (2H, d, $J = 8.4$ Hz, ArH-3',5'); MS m/z (%) 427.4 (M + 1, 100). **7g**: yield 33%, white solid, mp 140.9–142.9 °C; ^1H NMR (CDCl_3) δ ppm 1.28 (6H, d, $J = 6.4$ Hz, $2 \times \text{CH}_3$), 2.14 (6H, s, $2 \times \text{CH}_3$), 3.81 (1H, q, $J = 6.4$ Hz, CH), 4.69 (2H, s, ArCH₂), 5.53 (1H, s, NH), 5.96 (1H, s, ArH-6), 6.53 (2H, d, $J = 8.4$ Hz, ArH-2',6'), 7.04 (1H, s, ArH-3), 7.38 (2H, s, ArH-3'',5''), 7.40 (2H, d, $J = 8.4$ Hz, ArH-3',5'); MS m/z (%) 427.4 (M + 1, 100). **7h**: yield 34%, white solid, mp 161.0–162.8 °C; ^1H NMR (CDCl_3) δ ppm 2.14 (9H, s, $2 \times \text{CH}_3$, COCH₃), 3.55 (2H, s, NH₂), 5.29 (2H, s, ArCH₂), 5.52 (1H, s, NH), 6.00 (1H, s, ArH-6), 6.56 (2H, d, $J = 8.4$ Hz, ArH-2',6'), 6.94 (1H, s, ArH-3), 7.39 (2H, s, ArH-3'',5''), 7.42 (2H, d, $J = 8.4$ Hz, ArH-3',5'); MS m/z (%) 427.5 (M + 1, 62), 367 (M – 99, 100). **11a**: 50% yield, white solid, mp 170.5–172.0 °C; ^1H NMR (CDCl_3) δ ppm 2.13 (6H, s, $2 \times \text{CH}_3$), 3.54 (5H, s, OCH₃, NH₂), 4.67 (2H, s, CH₂O), 5.51 (1H, s, NH), 5.79 (1H, d, $J = 16.4$ Hz, =CH), 6.03 (1H, s, ArH-6), 6.55 (2H, d, $J = 8.8$ Hz, ArH-2',6'), 6.99 (1H, s, ArH-3), 7.17 (2H, s, ArH-3'',5''), 7.31 (2H, d, $J = 16.4$ Hz, CH=), 7.40 (2H, d, $J = 8.8$ Hz, ArH-3',5'); MS m/z (%) 425.3 (M + 1, 100). **11b**: 35% yield, white solid, mp 194.1–195.9 °C; ^1H NMR (CDCl_3) δ ppm 2.14 (6H, s, $2 \times \text{CH}_3$), 2.15 (3H, s, CH₃CO), 3.53 (2H, s, NH₂), 5.30 (2H, s, ArCH₂O), 5.51 (1H, s, NH), 5.78 (1H, d, $J = 16.8$ Hz, =CH), 6.05 (1H, s, ArH-6), 6.55 (2H, d, $J = 8.8$ Hz, ArH-2',6'), 6.93 (1H, s, ArH-3), 7.17 (2H, s, ArH-3'',5''), 7.30 (1H, d, $J = 16.8$ Hz, CH=), 7.40 (2H, d, $J = 8.8$ Hz, ArH-3); MS m/z (%) 393.2 (M – 59, 100), 453.3 (M + 1, 97.2). **12a**: 79% yield, white solid, mp 103.6–104.8 °C; ^1H NMR (CDCl_3) δ ppm 2.09 (6H, s, $2 \times \text{CH}_3$), 2.61 (2H, t, $J = 7.2$ Hz, CH₂CN), 2.87 (2H, t, $J = 7.2$ Hz, ArCH₂), 3.52 (3H, s, OCH₃), 4.67 (2H, s, CH₂O), 5.56 (1H, s, NH), 6.03 (1H, s, ArH-6), 6.55 (2H, d, $J = 8.8$ Hz, ArH-2',6'), 6.92 (2H, s, ArH-3'',5''), 6.99 (1H, s, ArH-3), 7.39 (2H, d, $J = 8.8$ Hz, ArH-3',5'); MS m/z (%) 427.3 (M + 1, 100). **12b**: 40% yield, white solid, mp 164.1–165.7 °C; ^1H NMR ($\text{DMSO}-d_6$) δ ppm 2.04 (6H, s, $2 \times \text{CH}_3$), 2.09 (3H, s, COCH₃), 2.78 (4H, s, $2 \times \text{CH}_2$), 4.58 (2H, s, NH₂), 5.19 (2H, s, CH₂O), 5.90 (1H, s, NH), 6.54 (2H, d, $J = 8.8$ Hz, ArH-2',6'), 6.87 (1H, s, ArH-6), 7.04 (2H, s, ArH-3''5''), 7.45 (2H, d, $J = 8.8$ Hz, ArH-3',5'), 8.08 (1H, s, ArH-3); MS m/z (%) 395.2 (M – 59, 100), 455.3 (M + 1, 17).

16. Jabeen I, Pleban K, Rinner U, Chiba P, Ecker GF. *J Med Chem.* 2012; 55:3261. [PubMed: 22452412]
17. Keserü GM, Makara GM. *Nat Rev Drug Discovery.* 2009; 8:203.
18. Ramurthy S, Subramanian S, Aikawa M, Amiri P, Costales A, Dove J, Fong S, Jansen JM, Levine B, Ma S, McBride CM, Michaelian J, Pick T, Poon DJ, Girish S, Shafer CM, Stuart D, Sung L, Renhowe PA. *J Med Chem.* 2008; 51:7049. [PubMed: 18942827]
19. Ishikawa M, Hashimoto Y. *J Med Chem.* 2011; 54:1539. [PubMed: 21344906]
20. Veber DF, Johnson SR, Cheng HY, Smith BR, Ward KW, Kopple KD. *J Med Chem.* 2002; 45:2615. [PubMed: 12036371]
21. Tarcsay A, Nyiri K, Keserü GM. *J Med Chem.* 2012; 55:1252. [PubMed: 22229549]



	EC ₅₀ (nM)		WS (ug/mL)		F%
	NL4-3	RTMDR1	2.0	7.0	
2a	3.00	ND	0.42	0.47	ND
2b	0.33	0.87	0.29	0.29	ND
2c	0.53	0.36	20.9	3.23	6.1

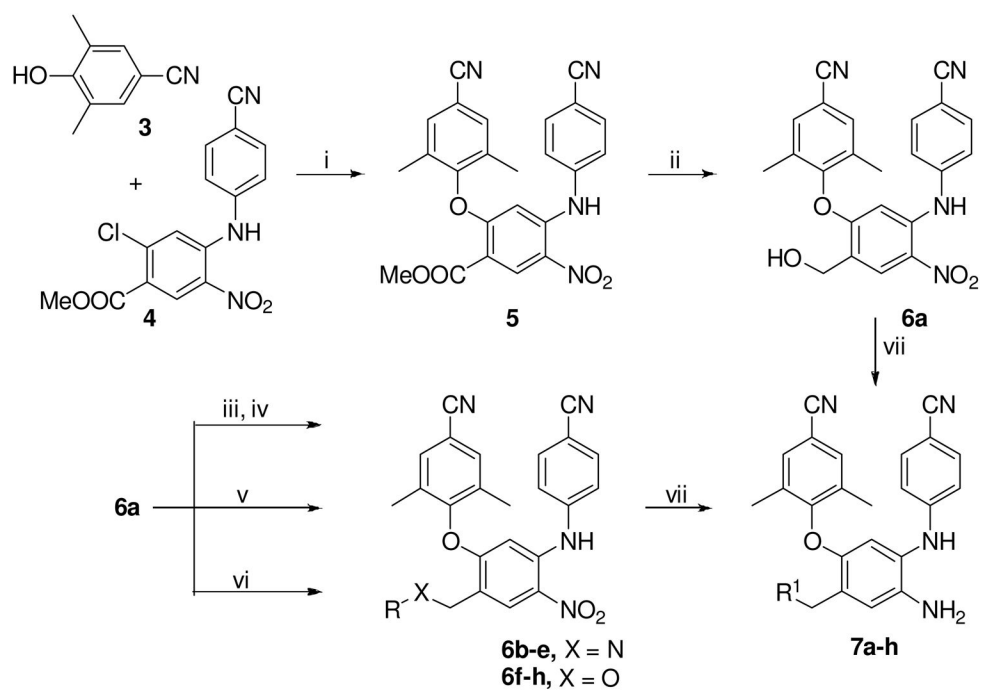
DAANs

2a R¹ = NO₂, R² = CN;
2b R¹ = NO₂, R² = (*E*)-CH=CHCN
2c R¹ = CH₂OH, R² = (*E*)-CH=CHCN

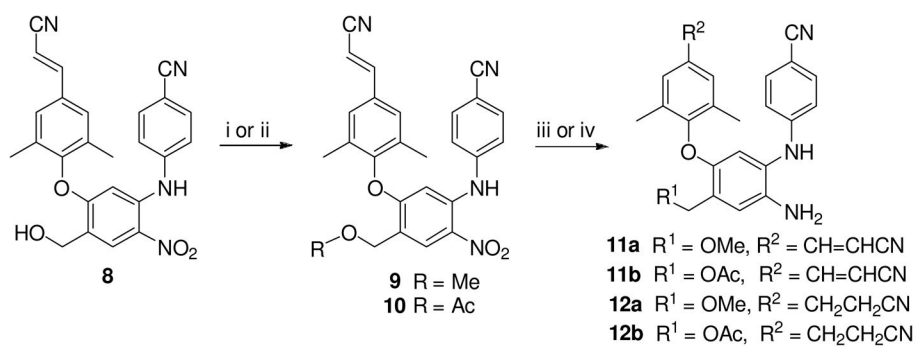
optimization →

New DAANs:
7 R² = CN
11 R² = (*E*)-CH=CHCN
12 R² = CH₂CH₂CN

Figure 1. Next-generation NNRTI drugs, diarylaniline leads (DAANs), and new DAAN analogues

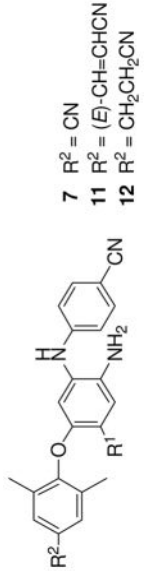
**Scheme 1.**

i) $\text{K}_2\text{CO}_3/\text{DMF}$, 120 °C, 6 h; ii) LiBH_4 , THF/MeOH, 0 °C, 7 h; iii) 2,4,6-trichloro-[1,3,5]triazine, DMF/ CH_2Cl_2 , rt, 4 h; iv) amine, THF, 0 °C, 0.5 h; v) ROH/ BiCl_3 , $\text{CH}_2\text{Cl}_2/\text{CCl}_4$, rt, 4 h; (vi) Ac_2O , 100 °C, Microwave, 5 min; vii) $\text{H}_2/\text{Pd-C}$ in EtOAc or EtOH.

**Scheme 2.**

i) ROH/BiCl₃, CH₂Cl₂/CCl₄, r.t. 4 h; ii) Ac₂O, 100 °C, Microwave, 5 min; iii) Fe, NH₄Cl, THF/MeOH/H₂O, reflux, 3 h; iv) H₂/Pd-C in EtOH.

Table 1

Anti-HIV data of new DAANs against wild-type and resistant viral strains^a


7 R² = CN
11 R² = (E)-CH=CHCN
12 R² = CH₂CH₂CN

R ¹	EC ₅₀ (mM) IIIB ^b	CC ₅₀ (μM)	SI	EC ₅₀ (mM) AI7 ^c	FC ^d
7a OH	1.07 ± 0.25	122	114,019	33.1 ± 4.05	30.9
7b NHMe	9.94 ± 1.57	12.7	1,278	115 ± 3.10	11.6
7c NHCH(CH ₂) ₂	10.6 ± 0.64	12.1	1,142	130 ± 2.87	12.3
7d NH(CH ₂) ₃ OH	6.10 ± 1.10	15.1	2,475	>2000	>328
7e N(CH ₂ CH ₂) ₂ NMe	170 ± 5.60	96.9	570	>2000	>11.8
7f OCHMe ₂	14.0 ± 1.10	89.4	6,386	315 ± 25.7	22.5
7g OMe	3.54 ± 0.62	146	41,243	298 ± 133	84.2
7h OAc	1.06 ± 0.01	113	106,604	374 ± 111	353
11a OMe	5.74 ± 2.20	50.3	8,763	14.7 ± 0.74	2.6
12a OMe	3.25 ± 0.23	>200	>61,538	2.95 ± 0.50	0.91
11b OAc	0.82 ± 0.07	96.3	117,439	36.50 ± 1.78	44.5
12b OAc	0.96 ± 0.12	44.8	46,667	4.92 ± 0.12	5.1
1b TMC278	0.49 ± 0.17	90.7	185,102	9.03 ± 0.74	18.4

^aExperiments performed at least in triplicate in MT-2 cells and data presented as the mean ± SD.^bHIV-1 wild-type virus.^cDrug-resistant virus from NIH with mutated K103N and Y181C in the NNRTI binding pocket.^dFold change resistance.

Table 2

Physicochemical parameters of new active DAAN compounds

	Aqueous solubility ($\mu\text{g/mL}$) ^d		mp °C	Log p ^b pH 7.4	clogD ^c	rPSA ^d (\AA^2)	Lipophilic efficiency indices ^{16,17}			
	pH 2.0	pH 7.4					pEC ₅₀ ^e	LE ^f	LLE ^g	LELP ^h
7a	9.12	0.86	230–2	3.57	3.23	115.1	8.97	0.42	5.40	8.50
7b	2.63	1.59	202–3	1.86	3.72	106.9	8.00	0.37	6.14	5.03
7c	2.86	13.0	72–3	3.84	4.08	106.9	7.97	0.34	4.13	11.30
7d	2.90	23.6	76–8	1.81	3.31	127.1	8.21	0.34	6.40	5.32
7g	3.75	0.07	176–8	3.84	4.16	104.1	8.45	0.39	4.61	9.85
7h	16.7	0.20	161–3	4.40	4.12	121.2	8.97	0.38	4.57	11.60
11a	1.70	0.11	171–2	4.13	4.48	104.1	8.24	0.35	4.11	11.80
12a	1.82	0.66	104–5	3.25	3.87	104.1	8.49	0.36	5.24	9.03
11b	1.87	0.49	194–6	4.48	4.45	121.2	9.08	0.37	4.60	12.20
12b	2.63	1.86	164–6	2.84	3.84	121.2	9.02	0.36	6.18	7.92
1b	86.8	0.24	246–8	> 5	3.62	97.4	9.31	0.46	5.69 ⁱ	7.87 ⁱ

^{a, b} Measured by HPLC in triplicate.^c Predicted by ACD software.^d Topological polar surface area predicted by ChemDraw Ultra 12.0.^e Negative logarithm values of potency converted from experimental data against wild-type virus IIB shown in Table 1.^f Calculated by the formula $-G/\text{HA}$ (non-hydrogen atom), in which normalizing binding energy $G = -\text{RT} \ln K_d$, presuming $\text{EC}_{50} \approx K_d$.^g Calculated by the formula $\text{pEC}_{50} - \log P$.^h Defined as a ratio of measured log P and LE.ⁱ Data calculated with clog D.